Massive Stars Near and Far
Proceedings IAU Symposium No. 361, 2024
J. Mackey, J. S. Vink, & N. St-Louis, eds.
doi:10.1017/S1743921322002642

Fundamental Properties of O and B Stars with Optical Interferometry

Kathryn D. Gordon[1], **Douglas R. Gies**[2] **and Gail H. Schaefer**[3]

[1]University of Tampa
401 W. Kennedy Blvd., Tampa, FL, USA
email: kgordon@ut.edu

[2]Georgia State University
CHARA, Department of Physics and Astronomy, Atlanta, GA, USA
email: dgies@gsu.edu

[3]The CHARA Array
Mount Wilson, CA, USA
email: gschaefer@gsu.edu

Abstract. We used interferometric observations made with the CHARA Array of 25 B-type stars and 6 O-type stars to obtain precise measurements of angular size, radius, and effective temperature to test stellar atmospheric models for massive stars. Our measured angular diameters range from 1.09 milli-arcseconds (mas) for β Tau down to 0.11 mas for 10 Lac, the smallest star yet resolved with the CHARA Array. The rotational oblateness of the rapidly rotating star ζ Oph is directly measured for the first time. We collected ultraviolet to infrared spectrophotometry for all sample stars and derived temperatures, angular diameters, and reddening estimates that best fit the spectra. There is generally good agreement between the observed and spectral fit angular diameters for the O and B stars, indicating that the fluxes predicted from model atmospheres are reliable. The derived and model temperatures for the O stars are also in fair agreement, however the sample size is small and several of the O stars results we consider to be preliminary. On the other hand, the temperatures derived from angular diameters and fluxes tend to be larger (by $\approx 4\%$) for the B stars than those from published results based on analysis of the line spectrum (Gordon et al. 2018, 2019).

Keywords. stars: early-type, stars: fundamental parameters (classification, colors, luminosities, masses, radii, temperatures, etc.), techniques: interferometric

1. Introduction

Massive stars have a critical impact on their surroundings due to their intense radiation, strong stellar winds and explosive ends as supernovae. They are also the progenitors of many interesting astrophysical objects, from black holes to Wolf-Rayet stars and Luminous Blue Variables. It is therefore important to have an accurate understanding of the parameters of these stars and how these parameters relate to their evolutionary state. Fundamental parameters such as radius and effective temperature, for individual O and B-type stars are generally determined through continuum flux measurements or by detailed analysis of the line spectrum. The determination of fundamental parameters of individual O-type stars is mostly based on analysis of the line spectrum, in which the temperature and gravity are derived from the He line ionization balance and the pressure broadening of the hydrogen lines. For the hot and intermediate-mass B-type stars an estimation of effective temperature is generally found by continuum flux measurements

https://doi.org/10.1017/S1743921322002642 Published online by Cambridge University Press

or by detailed analysis of the line spectrum. Both of these methods rely on comparisons with predictions from stellar model atmospheres. It is therefore of critical importance to test these models through independent means.

With long-baseline optical interferometry, we are able to resolve the disks of these stars and directly measure their angular diameters. This can be combined with a known distance, from *Gaia* parallax measurements (Gaia Collaboration et al. 2018), to obtain an independent determination of the radius of the star. The effective temperature is derived from the relationship between the extinction corrected bolometric flux, angular diameter θ, and $T_{\rm eff}$:$f_{\rm bol} = \frac{1}{4}\theta^2\sigma T_{\rm eff}^4$. We can then compare our observationally determined angular diameters and effective temperatures to those predicted by stellar atmosphere models to test their validity. Once physical radii and effective temperatures are determined, stars can be plotted on an observational HR diagram and age estimates can be obtained from model isochrones. We have utilized the TLUSTY OSTAR 2002 (Hubeny & Lanz 1995; Lanz & Hubeny 2003), the TLUSTY BSTAR2006 (Lanz & Hubeny 2007), and the ATLAS9 (Kurucz 1992; Castelli & Kurucz 2004) models as the temperature of each star dictated. The TLUSTY models are non-LTE (non-local thermal equilibrium), which becomes more important in hotter atmospheres, and the ATLAS9 models are LTE. All models assumed solar abundances.

In these proceedings, we present the results of our angular diameter measurements of a sample of 25 B stars and 6 O stars. We discuss the fits of the SED as a function of temperature, angular size, and reddening for each star, and the comparison of observed and derived parameters to model predictions. More detailed discussions of these studies can be found in their respective papers, with the O star results in Gordon et al. (2018) and the B star results in Gordon et al. (2019).

2. Observations

The stars in our observational sample consisted of six O spectral type stars ranging from O7.5 to O9 and 25 B-type stars with spectral types ranging from B2 to B9. All luminosity classes are represented with 3 supergiants, 16 giants, one sub-giant, and 11 dwarfs, or main sequence stars. All target stars had a V magnitude of 5 or less and had a predicted angular diameter range of 0.21.0 mas. Choosing stars with these constraints on brightness, size, and with a declination of greater than $-14°$ ensured that they would be observable and resolvable with the CHARA Array. All O star observations were made using the Precision Astronomical Visible Observations (PAVO) beam combiner (Ireland et al. 2008) at the CHARA Array (ten Brummelaar et al. 2005), located at Mount Wilson Observatory in California. B stars were observed with PAVO or with the CLassic Interferometry with Multiple Baselines (CLIMB) beam combiner (ten Brummelaar et al. 2013) as their predicted angular sizes dictated.

The CHARA Array is an optical interferometer composed of six 1m telescopes arranged in a Y-shaped configuration. Combinations of the telescopes allow for 15 different usable baselines ranging in length from 34 to 331 m. Combining the longest usable baseline currently available in the world and the operating wavelength range of the PAVO beam combiner (650800 nm), we were able to achieve an extremely high angular resolution for our targets of about 0.2 mas. The CLIMB beam combiner was operated in the H-band (1.67 μm) and has a resolution limit of about 0.5 mas.

Because of their shorter lifetimes, it is common for massive stars to have a close companion or be a member of a multiple star system. The extra flux from these companions can affect the fitting of our interferometric data and spectophotometric modeling and must be accounted for. A literature search was done for each target star to uncover known companions. Targets with companions close enough to contribute incoherent flux in the

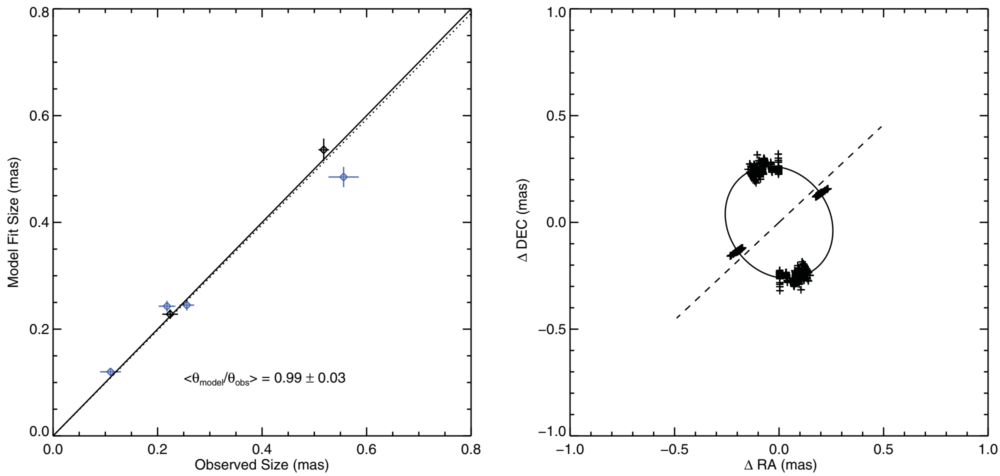

Figure 1. (a) (Left) Observed angular size θ_{LD} compared to the angular size $\theta_{LD}(T_{\rm eff})$ derived from the published $T_{\rm eff}$ and fit to the SED for the O star sample. The solid line shows a line with a slope of unity for reference, and the dashed line shows the trend for the mean ratio of these diameters. Blue points indicate diameter estimates based upon only a single data bracket or an extremely small angular size in the case of 10 Lac. From Gordon et al. (2018).
Figure 1. (b) (Right) A simple ellipse fitted to our interferometric data for ζ Oph. Each symbol shows the derived angular size of a limb-darkened star whose visibility equals the observed value, and each is plotted at a position angle derived from the (u, v) spatial frequencies of the observation. The fit was made of the major and minor axes with the position angle of the minor axis set by published polarimetry. The dashed line shows the adopted rotational axis of the star at a position angle of $132.^\circ 5$. From Gordon et al. (2018).

field of view of the detector were corrected with the method described in Boyajian et al. (2008) for the interferometric data and by adding the calculated flux of the companion to the spectrum for the spectrophotometric modeling.

3. Results

3.1. *O Stars*

Our initial survey of O stars finds that the measured diameters are generally in good agreement with the expected diameters based upon the published temperatures and model fits of the SED. A comparison of observed $\theta_{\rm LD}$ (limb-darkened angular diameter) and the predicted angular size $\theta_{\rm LD}(T_{\rm eff})$ is shown in Figure 1.(a) with the average ratio of $\theta_{\rm LD}(T_{\rm eff})$ to $\theta_{\rm LD}$ as approximately 0.99 ± 0.03. Two evolved stars in our sample, ξ Per and ζ Ori A, do not fit with model predictions as well but have limited data coverage and we consider these results preliminary. Additional interferometric observations are needed to confirm the diameters found in these cases and the O star sample needs to be expanded to give greater statistical significance to our results and allow us to investigate effective temperature trends.

ζ Oph is a particularly interesting O star with an extremely rapid rotational velocity. It has an estimated $v \sin i$ of 311 km/s (Simón-Díaz et al. 2014), or about 90% of its critical velocity (Howarth & Smith 2001). We observed ζ Oph on two different baselines with different position angles to measure its oblateness due to its rapid rotation. By setting the position angle from a past spectropolarimetric study (Poeckert et al. 1979), we made an elliptical fit to the diameter as a function of position angle in the sky determined from our observations. This fit is shown in Figure 1.(b) and constitutes the first direct measurement of the shape of ζ Oph.

https://doi.org/10.1017/S1743921322002642 Published online by Cambridge University Press

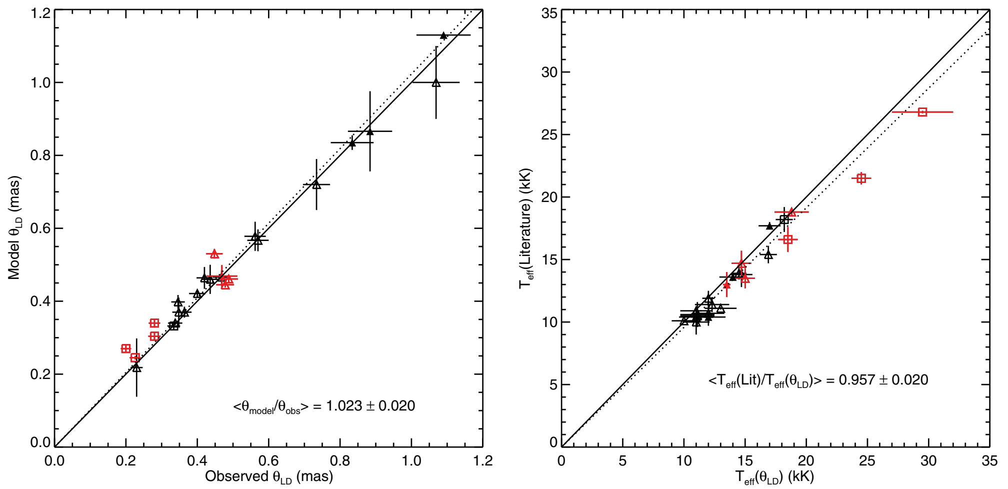

Figure 2. (a)(Left) A comparison of our observed angular diameters to the SED-derived model size for the B star sample. The solid line is a unit slope line for reference, and the dotted line indicates the weighted mean of $\theta_{model}/\theta_{obs}$. Square symbols indicate stars fit with the TLUSTY BSTAR2006 models, triangles indicate stars fit with ATLAS9 models, and filled triangles indicate stars with CLIMB data. Red points are measurements considered preliminary and are not included in the weighted mean ratio shown. From Gordon et al. (2019).
Figure 2.(b) (Right) A comparison of our derived temperatures to the average literature temperature $T_{\rm eff}$(Lit) for the B star sample. The solid line is a unit line for reference and the dotted line indicates the weighted mean of the ratio of variables being compared. Square symbols indicate stars fit with the TLUSTY BSTAR2006 models, triangles indicate stars fit with ATLAS9 models, and filled triangles indicate stars with CLIMB data. Red points are measurements considered preliminary and are not included in the weighted mean ratios shown. From Gordon et al. (2019).

3.2. *B Stars*

The results of our angular diameter survey of 25 B stars found that our measured angular diameters are in good agreement with model predicted angular sizes. This result does set aside some observed stars with data we consider preliminary due to complications discussed in detail in our B star paper (Gordon et al. 2019). A comparison of measured and model angular diameters is shown in Figure 2.(a). Our derived interferometric effective temperatures are also in good agreement with the model predicted effective temperatures. This agreement confirms the validity of the application of the TLUSTY (Lanz & Hubeny 2007) and ATLAS9 (Kurucz 1992; Castelli & Kurucz 2004) stellar atmosphere models for most main-sequence B-type stars. However, there is some discrepancy between our derived effective temperatures and those determined primarily from spectral line studies. A comparison of these two $T_{\rm eff}$ measurements is shown in Figure 2.(b), and the error weighted average ratio is $< T_{\rm eff}(\mathrm{Lit})/T_{\rm eff}(\theta_{LD}) >= 0.957 \pm 0.022$ after removal of the preliminary results. This represents a 2σ smaller estimate for $T_{\rm eff}$ from line studies compared to that from the continuum SED fit at the observed angular size.

Another notable discrepancy in our B star sample comes from our observations of 55 Cyg, the only supergiant in our sample. The observed angular size, at 0.448 ± 0.023 mas, is 15% smaller than the model prediction, 0.530 ± 0.013 mas, which leads to a best fit temperature of 18.8 ± 1.4 kK, which is 14% higher than the model fit value of 16.5 ± 1.0 kK. However, a previous spectral study of 55 Cyg by Kraus et al. (2015) using the FASTWIND stellar atmosphere code (Santolaya-Rey et al. 1997) found an effective

https://doi.org/10.1017/S1743921322002642 Published online by Cambridge University Press

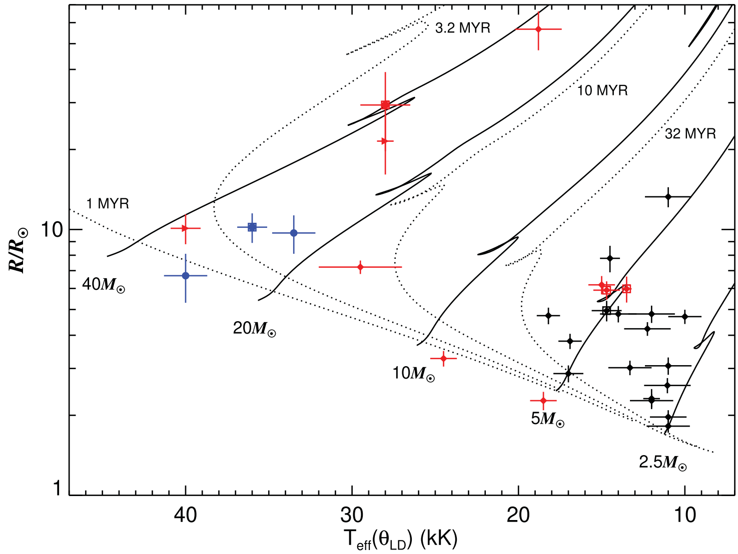

Figure 3. Observational HR diagram for our targets based on our observed diameters and derived effective temperatures. The black diamonds indicate B stars, blue circles O stars, and triangles are O stars with only upper or lower effective temperature estimates. Red points indicate results we consider to be preliminary. Symbols enclosed by squares indicate stars that are cluster members. Evolutionary tracks and isochrones are from the MESA grid. From Gordon et al. (2019).

temperature of 18.8 kK, which is in excellent agreement with our derived temperature. Kraus et al. (2015) also gives a stellar radius for 55 Cyg of $57R_\odot$, which when combined with the distance from the recent *Gaia* DR2 parallax (Gaia Collaboration et al. 2018), gives an angular diameter of 0.45 ± 0.07 mas. This is in good agreement with our measured angular diameter. We suspect that this discrepancy is due to the fact that the TLUSTY BSTAR2006 and ATLAS9 models do not incorporate the effects of stellar winds, which can be quite significant for massive supergiant stars. It will be important to compare interferometric results and fluxes of the supergiants to models like CMFGEN (Hillier & Miller 1998), and we are working on studying this effect with a sample of B supergiants.

We combined our observed angular diameters with known distances to calculate stellar radii. *Gaia* DR2 parallaxes were used to calculate distance where available. If no *Gaia* DR2 parallax was available, then the Hipparcos (van Leeuwen 2007) value was adopted. With our derived estimates for stellar radius and effective temperature, we placed our sample stars on an observational HR diagram. This is shown in Figure 3, and includes the O star and B star sample. Circles indicate the O stars, while the triangles mark the two O stars for which we only have upper or lower limits on $T_{\rm eff}$. Overplotted are evolutionary tracks and isochrones for the MESA grid (Paxton et al. 2013; Choi et al. 2016; Dotter 2016). This allows for stellar age and mass estimates that are observationally defined and less model dependent than previous methods.

References

Boyajian, T. S. et al. 2008, ApJ, 683, 424

Castelli, F., & Kurucz, R. L. 2004, ArXiv Astrophysics e-prints

Choi, J., Dotter, A., Conroy, C., Cantiello, M., Paxton, B., & Johnson, B. D. 2016, ApJ, 823,